Miniature photometric stereo system for textile surface structure reconstruction

Dimitris Gorpas*[,a,b], Christos Kampouris[a] and Sotiris Malassiotis[a]

[a]Information Technologies Institute, Centre for Research and Technology - Hellas, Thessaloniki, GR 57001, Greece;
[b]Department of Biomedical Engineering, University of California, Davis, CA 95616, USA

ABSTRACT

In this work a miniature photometric stereo system is presented, targeting the three-dimensional structural reconstruction of various fabric types. This is a supportive module to a robot system, attempting to solve the well known "laundry problem". The miniature device has been designed for mounting onto the robot gripper. It is composed of a low-cost off-the-shelf camera, operating in macro mode, and eight light emitting diodes. The synchronization between image acquisition and lighting direction is controlled by an Arduino Nano board and software triggering. The ambient light has been addressed by a cylindrical enclosure. The direction of illumination is recovered by locating the reflection or the brightest point on a mirror sphere, while a flat-fielding process compensates for the non-uniform illumination. For the evaluation of this prototype, the classical photometric stereo methodology has been used. The preliminary results on a large number of textiles are very promising for the successful integration of the miniature module to the robot system. The required interaction with the robot is implemented through the estimation of the Brenner's focus measure. This metric successfully assesses the focus quality with reduced time requirements in comparison to other well accepted focus metrics. Besides the targeting application, the small size of the developed system makes it a very promising candidate for applications with space restrictions, like the quality control in industrial production lines or object recognition based on structural information and in applications where easiness in operation and light-weight are required, like those in the Biomedical field, and especially in dermatology.

Keywords: Photometric stereo, focus measure, surface reconstruction, textile structure

1. INTRODUCTION

One of the most stimulating challenges in the field of robotics is the solution of the "laundry problem". This is the development of a robotic system that can navigate in unstructured environments, identify and remove textiles from piles or containers, and finally untangle and spread the textiles for some industrial process or folding, just like a human would do.[1] A very important aspect of this problem is the successful classification of the various fabric types, through means of computer vision. Due to the uneven surface, which is made by the yarn structure, the reflection of light affects the appearance of texture on the fabric surface. Its structural classification, based on a single image, is thus quite ambiguous and subject to the scene lighting conditions. Therefore, other techniques for the extraction of the fabric structural features have been investigated over the last few years. One of these techniques includes the acquisition of multiple images from the same viewpoint, but under varying illumination directions, and the three-dimensional reconstruction of the fabric surface.[2,3]

This is a very promising approach for the extraction of the fabric structural features, mostly because it is independent of complex surface color and texture variations. It is widely known as photometric stereo and was introduced by R.J. Woodham in the early 1980s.[4] Since then, photometric stereo has been exploited in a great extend and numerous approaches and systems are available in literature.[5–7] Photometric stereo is a method that can recover the orientation and reflectance properties of the inspected surface.[8] This method has the advantage, over conventional stereo vision, that is does not incorporate the solution of the correspondence problem and thus it allows the per pixel surface reconstruction with significant time efficacy and reduced computational requirements.

* dgorpas@ucdavis.edu; phone 1 530 754-6586

Videometrics, Range Imaging, and Applications XII; and Automated Visual Inspection, edited by Fabio Remondino, Mark R. Shortis, Jürgen Beyerer, Fernando Puente León, Proc. of SPIE Vol. 8791, 879117
 · doi: 10.1117/12.2018913

However, the majority of the research in this field, nowadays, targets to relatively large-scale problems. Some examples include the reconstruction of various artifacts,[9–12] and the acquisition of three-dimensional human models,[13–15] especially for creating avatars to populate virtual environments and for facial encoding and recognition. On the other hand, and to the authors knowledge, there exist a limited number of works available in literature that target close-range surface reconstruction, based on photometric stereo, and especially for objects with approximately 1 cm maximum diameter and a few millimeters maximum height.[16,17]

Although some of these systems can be used or have been used for the three-dimensional reconstruction of textile surfaces,[18] their relatively large dimensions and/or their requirement of controlled environmental lighting conditions prohibit their incorporation to a robotic system capable of operating in totally uncontrolled environments.

The development of a miniature photometric stereo system, which can be mounted on a robotic gripper and used for the extraction of the fabric structural features, has been the main objective of this paper. The small size of the developed system is the major contribution of this work. Moreover, its impact is further increased through the enhancement of the system with a metric that assesses the image focus quality and provides a feedback that can be used to appropriately guide the gripper. In order to address the ambient light interaction with the measurements, the developed system is enclosed into a cylindrical tube. That way, there is no need for controlled environmental lighting conditions, since the inspected surface is always isolated from the presence of the ambient light. In the current version of the system, the classical photometric stereo technique is applied,[4] considering a Lambertian surface for the textiles[8] in order to recover the three-dimensional surface normals, while the Frankot-Chellappa integration method[19] is used for the depth data recovery.

The rest of the paper is organized as follows. In Section 2 brief descriptions of the developed system and the applied photometric stereo technique are presented. In this section, the used focus metric is also described. The functionality of the system is discussed in Section 3, where the three-dimensional reconstruction of various fabric types is also presented. Finally, the paper concludes with a short discussion on the contribution of this work and the prospects of the developed system.

2. MATERIALS AND METHODS

In its current state, the system is consisted of a lab prototype photometric stereo module and the corresponding software, which is based on the classical approach of surface three-dimensional reconstruction through photometric stereo measurements. In the following sections both of these elements will be briefly described and the challenges encountered for will be discussed.

2.1 Miniature photometric stereo system

The basic concept of photometric stereo theory is that the surface orientation of the inspected scene can be addressed by acquiring several images of the scene, under the same viewpoint, but with varying illumination directions.[4] Of course this concept is not totally unconstrained. In fact several constrains exist, with the two most important being the assumption of orthographic image projection and the existence of a point source, located at a distance from the sensor. For all these assumptions there exist an intense scientific interest on how they can be relaxed or bypassed and yet achieve accepted levels of reconstruction accuracy.[8] Towards the development of the miniature photometric stereo system, which is presented in Fig. 1, effort has been placed on the fulfilment, to the greatest extent, of these assumptions.

Figure 1. Front view (left), side view (right) and cross-sectional view (middle) of the lab prototype photometric stereo system.

The miniature system, as it can be observed in Fig. 1, consists of a low-cost off-the-self web-camera, eight light emitting diodes (LEDs) and a cylindrical enclosure. The camera that was selected presents a video graphics array (VGA) image resolution, which is 640×480 pixels, and its physical dimensions are approximately 32.2 mm width, 27.7 mm height and 28.1 mm depth, Fig. 2a. As it is expected, such a camera is not based on an orthographic image projection, but instead it is strongly characterized by a perspective mode for image formulation. Moreover, with such a camera it is impossible to succeed the desired magnification for the textile structure extraction, when restricted to the focus range permitted by the manufacturer.

However, the camera is equipped with a manual focus functionality, which implies that it is possible to place the lens at such a distance from the sensor, where macro operation is almost feasible. Through this modification an approximate orthographic projection is succeeded, satisfying one of the aforementioned photometric stereo assumptions. Indeed, by moving the lens further away from the sensor and closer to the inspected scene, mostly the perpendicular light rays contribute to the image formulation. The shortcomings of such a modification are (a) that more light is required for the image formulation, since mostly the perpendicular rays contribute, and (b) the image corners are blurry due to the very shallow depth of field and their larger distance from the camera sensor. Two examples of fabric acquisition are shown in Fig. 2b and Fig. 2c. The first one is from the camera with the lens positioned within the focus range permitted by the manufacturer and the second one with the lens positioned further away from the camera sensor.

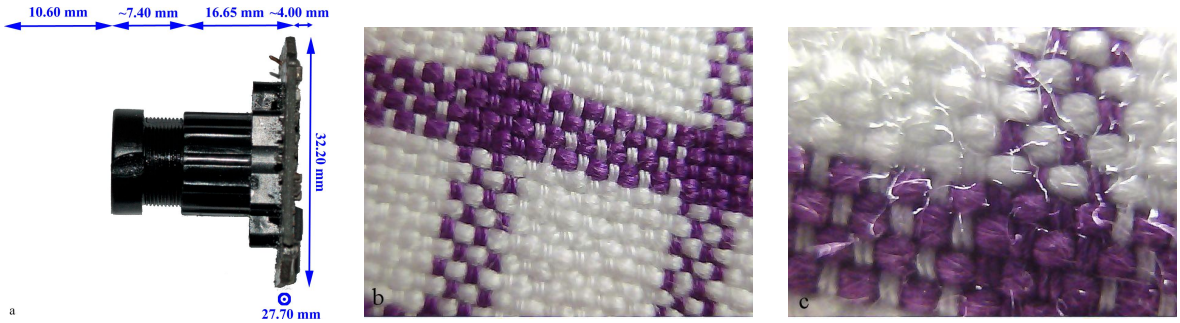

Figure 2. The physical dimensions of the camera board (a) and two examples of textile acquisition with the lens positioned within the focus range permitted by the manufacturer (b) and at macro mode operation (c).

The physical dimensions of the camera board were taken into account during the design of the camera housing. As it is obvious in Fig. 1, the camera housing is a cylindrical tube, made of light-weight plastic and painted matte black to reduce stray light within the tube due to internal reflections. The diameter of this tube was determined by the maximum diameter of the camera board, which, according to Fig. 2a, is approximately 42.5 mm. This diameter was further reduced by smoothing the edges of the camera board, as seen in Fig. 3a, succeeding a cylinder internal diameter equal to 35.0 mm and external diameter equal to 40.0 mm. On the other hand, the length of the cylinder was determined by the depth of the camera module and the desired working distance.

With the selected camera, as well as with any other camera equipped with manual focus, the imaging plane can be as close to the lens front side as there exist enough illumination for the image formulation. Thus two were the parameters considered for the extraction of the desired working distance. The illumination scheme was the first one. From literature it is known that the ideal photometric stereo illumination requires all lights, when uniformly distributed around the sensor, to have an approximate 55° zenith angle, relative to the image plane normal.[20] This assumption determines the distance that should also exist between two diametrically opposed lights and which is approximately equal to 3 times fold the working distance. The second parameter was the approximate field of view. Practical experience suggests that the maximum size of the fabrics pattern is in the order of 0.05 mm for fine fabrics, i.e. silk, and 0.5 mm for thick fabrics, i.e. thick coarse wool. Assuming these dimensions, in order to provide adequate information for the classification process, the pattern should be repeated within the inspected area at least 10 to 20 times. Moreover, in order to consider orthographic projection the acquired images were cropped to 400×400 pixels, discarding the problematic out of focus image corners. Thus the field of view should present a diameter in the order of 10.0 mm, which can provide the required information. A working distance of approximately 10.0 mm is adequate to provide the desired field of view and yet to provide

Table 1. The physical dimensions of the lab prototype photometric stereo system.

Dimension	Value
External diameter	40.0 mm
Internal diameter	35.0 mm
Length	39.9 mm
Sensor WxHxD	27.7x32.2x23.0 mm^3
Sensor diameter	34.5 mm
LED ring diameter	31.6 mm

Figure 3. The camera board with rounded corners (a), the lower part of the cylindrical tube with the camera mounted (b) and the light ring (c), all compared to 50-cent euro coin.

an approximate light ring diameter of 30.0 mm, which is smaller than the designed cylinder internal diameter. This value is presented in Fig. 2a and should be added to the camera depth in order to extract the length of the designed cylinder. In Table 1 the dimensions of the prototype system are presented, whereas further images of the various parts of the developed system are shown in Fig. 3b and Fig. 3c.

The illumination and its control was the final hardware aspect considered during the design of the lab prototype. As has been mentioned earlier in this section, one of the major assumptions of photometric stereo is that the light sources assumed to be point sources, placed at a large distance from the inspected area, so to safely consider uniform, almost collimated, illumination on the surface. However, this could not be assumed for the developed system, where the illumination sources are relatively close to the inspected area. To relax this prerequisite of photometric stereo, Fresnel lens have been added to the system, as shown in Fig. 3c, which are often used to collimate LEDs illumination. In Fig. 4 are presented two images acquired by the system, which show how uniformly the inspected area is illuminated under the use of the Fresnel lens, in contrary to a narrow-angle LED. Moreover, it is obvious in Fig. 4 that the problematic pixels corresponding to shadows or highlights are almost non existent in the first case, but they dominate the second one.

Taking into consideration the overall dimensions of the designed system, the illumination sources are 3 mm LEDs with corresponding Fresnel lenses. The constructed LED ring of Fig. 3c can hold at maximum 8 sources, equally distributed around the camera lens. Under the assumption of known albedo, 2 light sources are required to extract the surface orientation, while 3 are required to additionally estimate the albedo if it is not known. In order to compensate the absence of the ideal measurement conditions, more light sources are used, formulating

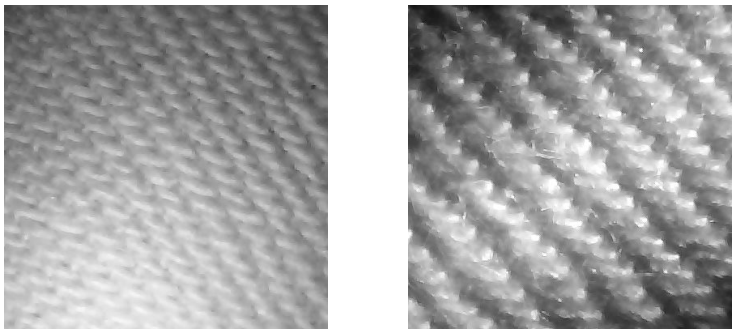

Figure 4. Difference in the illumination profile with (a) and without (b) the use of the Fresnel lens.

an optimization problem with its solution being an approximation of the actual surface structural characteristics. As it can be seen in Fig. 3c, the LED ring can be mounted on the camera lens, while in Fig. 5 are shown the various elements of the lab prototype. The lower part of the cylindrical tube can be removed and thus make it possible to handle the LED ring and/or adjust the focus of the system.

As it is shown in Fig. 5, the LEDs have not been permanently installed on the system, but they can easily be replaced. This is not only for maintenance reasons, such as to replace a diode, but also to try various wavelengths. Fabrics are quite diffusive materials, and with the addition of chemicals and colors they reflect light differently for each spectral band. In addition, that way the system can be used for other applications as well. For instance, the textiles can be reconstructed pretty well with white LEDs. White light, however, is strongly scattered by skin and is not applicable for skin reconstruction. Shorter wavelengths, closer to UV radiation, are required for optimum skin reconstruction.

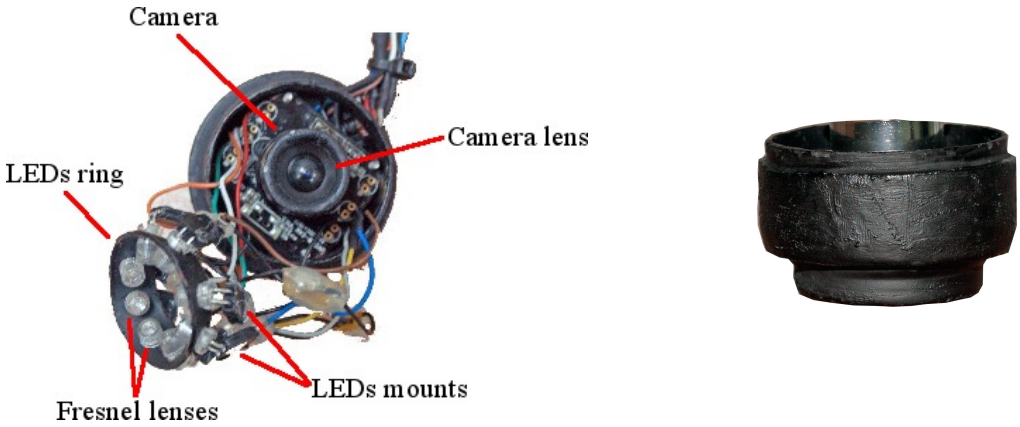

Figure 5. The various elements of the lab prototype (left) and the lower part of the cylindrical tube (right).

2.2 Photometric stereo algorithm

The solution to the surface three-dimensional reconstruction problem, from the images acquired with the lab prototype, was implemented through the classical photometric stereo theory and by considering textiles as Lambertian surfaces. According to this theory, the intensity for each pixel and for each illumination direction can be expressed as:[21]

$$I^k(u,v) = \rho_S(u,v) \cdot \vec{L}^k \cdot \vec{N}(u,v) \tag{1}$$

where $I^k(u,v)$ is the intensity value and $\rho_S(u,v)$ is the albedo at the pixel (u,v) of the k^{th} image $(k = 1, \cdots, 8)$ with unit vector normal to the surface $\vec{N}(u,v)$. This image has been acquired while the inspected surface was illuminated by the LED with direction $\vec{L}^k$. Eq. 1 can also be written in the form of matrices as:

$$\mathbf{I}(u,v) = \rho_S(u,v) \cdot \mathbf{L} \cdot \vec{N}(u,v) \tag{2}$$

where $\mathbf{I}(u,v) = \left[I^k(u,v)\right]$ and $\mathbf{L} = \left[\vec{L}^k\right]$. In the case that the illumination vectors are not co-planar, then the illumination matrix $\mathbf{L}$ is non-singular and can be inverted leading to the following expression:

$$\mathbf{M}(u,v) = \mathbf{L}^{-1} \cdot \mathbf{I}(u,v) \tag{3}$$

Eq. 3 is actually an optimization process for the solution of the problem in the form $\mathbf{A} \cdot \mathbf{X} = \mathbf{b}$, and results to the vector $\mathbf{M}(u,v) = [m_n(u,v)]$, $n = 1, \cdots, 3$. From this vector, the surface gradients can be extracted:

$$p_n(u,v) = -m_1(u,v)/m_3(u,v) \quad and \quad q_n(u,v) = -m_2(u,v)/m_3(u,v) \tag{4}$$

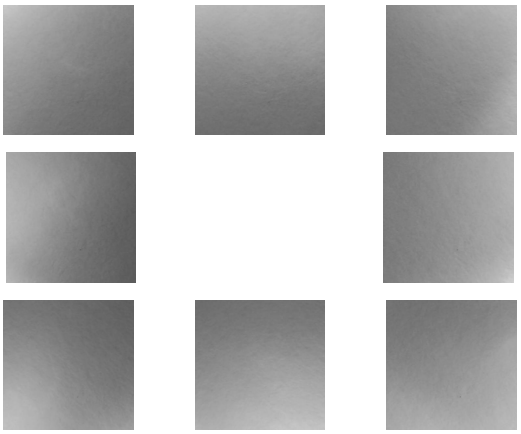

Figure 6. The flat-fielding images acquired from a white paper card for all the illumination directions.

as well as the surface albedo

$$\rho_S(u,v) = \sqrt{m_1^2(u,v) + m_2^2(u,v) + m_3^2(u,v)} \tag{5}$$

The depth map of the inspected surface can be recovered by integrating the surface gradients. To enforce integrability the Frankot-Chellappa algorithm was used.[19] The methodology described in Eq. 1 through Eq. 5 has as prerequisite that uniform illumination exists over the entire inspected surface. With such small working distance, however, the illumination cannot be uniform, even with a collimated light source, due to the inverse square law of light.[22] To confront this problem, a flat-fielding process precedes the photometric stereo algorithm. This process is actually a normalization of the acquired images with images acquired from a Lambertian surface, with known albedo, under the same illumination directions. In Fig. 6 are presented 8 gray-scale reference images from a gray paper card. These images have been used to normalize the acquired data that will be presented in the following section.

One other issue is the estimation of the illumination directions. This is succeeded by using a mirror sphere and detecting the center of the reflected highlight for each LED. In Fig. 7 are presented the acquired images from the mirror sphere used to extract the required directions. After finding the surface normals on the detected spots, the law of specular reflection is used to obtain the directions of the illumination sources.

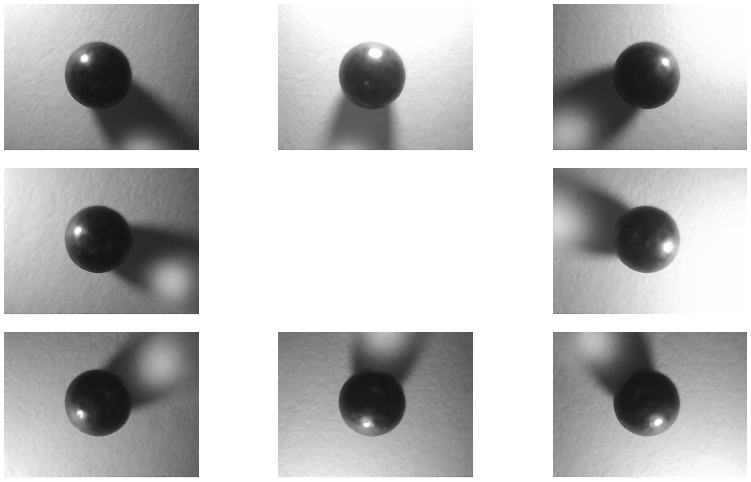

Figure 7. The mirror sphere under the 8 different illumination directions.

Finally, the illumination system is controlled by an Arduino Nano micro-controller board. The synchronization between the frame acquisition and illumination is achieved by software triggering the Arduino board. The micro-controller has been placed in a small mounting box and it communicates through USB port with the computational unit and through a 9-pin D-Sub connector with the photometric stereo system.

2.2.1 Focus measure

As it has been already mentioned, the developed system is characterized by a shallow depth of field, in the order of few millimeters. Consequently, it is essential to accurately estimate the image plane before initializing the image acquisition process. This is a functionality already provided by most cameras with automated focus adjustment and is used to drive the motor that controls the distance between the lens and the sensor. In the developed system this metric is required to control the working distance, since the focal length is manually fixed. The cylindrical enclosure of Fig. 5 defines the working distance, as it has been described in a previous section. However, when attached to the robot gripper it will become essential to provide a feedback to the controller of the robot so that it will properly guide the gripper without damaging either the photometric stereo system, the gripper or the inspected surface.

In order to succeed this, the Brenner's focus measure is estimated by the equation:[23]

$$F_{Brenner} = \frac{1}{M \cdot N} \cdot \sum_{M} \sum_{N} \left(g(i, j+2) - g(i, j)\right)^2 \tag{6}$$

where M and N are the dimensions of the region g where the focus measure is assessed. The region g can be equal to the entire image, or to a smaller region of interest. Moreover, Eq. 6 has been modified so to consider both horizontal and vertical differences and the maximum value at each coordinate was used to preform the sums. In case the region to evaluate the focus measure is relatively small, Eq. 6 can be addressed simultaneously with frame acquisition. Thus, this will be the parameter to properly guide the robot gripper in the desired position for optimum imaging.

3. RESULTS AND DISCUSSION

3.1 Focus measure

In Fig. 8 are presented two examples of the focus measure functionality. During the evaluation of this metric the scene is illuminated by four LEDs, uniformly distributed around the camera lens. The focus measure is estimated for every frame captured by the camera. The optimal focus is succeeded, as seen in Fig. 8, when the maximum value of this metric is recorded.

In the block diagram of Fig. 8 the basic structure of this functionality is shown. The initial measurements were implemented with the system being hand held, however the operation will be exactly the same when attached to the gripper. For every position an estimation of the focus measure is stored. When the maximum value is recorded, the corresponding gripper position is also available and can be sent back to the robot controller. The STOP criterion, in the examples of Fig. 8, was the extraction of the maximum value, followed by five sequential steps with smaller focus measures.

As it has been aforesaid, this measure can be evaluated real time, when the region of interest is relatively small. However, even if the entire image is considered, the estimation of this measure is very fast. More specifically, when considering the entire acquired image, 640×480 pixels, the Brenner's measure estimation required less than 0.01 sec per frame. This is significantly faster than the 58 sec required for the focus measure based on image contrast[24] and the 0.31 sec required by the sum of wavelet coefficients measure.[25] The Gaussian derivative method,[26] which is another well applied focus measure, required approximately 0.1 sec. Since the Brenner's focus measure is based on simple equations applied on each pixel value, it is significantly faster than the more complex measures reported in literature and yet it presents the same accuracy in selection of the optimal imaging plane.

For the comparison of the different focus metrics, all measurements have been performed on a quad-core system with 8 GB RAM.

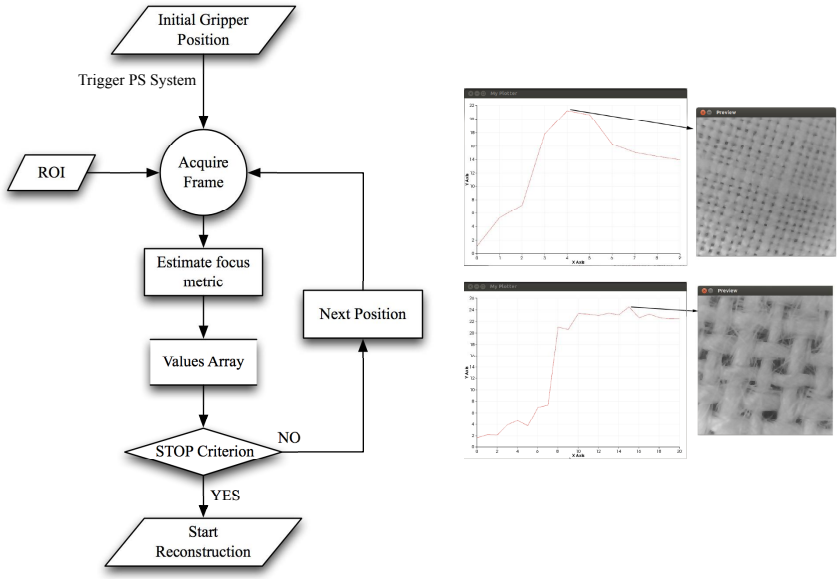

Figure 8. Block diagram of the focus measure estimation process (left) and two examples of its functionality (right).

3.2 Surface reconstruction

In this section, results from three-dimensional surface reconstruction of various fabrics will be presented. For all the following examples, LEDs emitting broadband white light have been used. The flat-fielding of the acquired images was realized by normalizing them with the corresponding images presented in Fig. 6. Finally, the surface reconstruction was implemented for a region of interest equal to 400×400 pixels, with its origin located at the center of the acquired image. Since color is not useful as a classification feature for textiles, all images were acquired in gray scale.

Fig. 9 shows the albedo and the point cloud of the reconstructed surface of the Yuta fabric. This textile is quite common in rugs and as it is shown in Fig. 9 is characterized by a coarse 1×1 plain weave pattern. The system has successfully reconstructed the weave pattern of the fabric, whereas the fixed working distance and the 400×400 pixels region of interest provide adequate pattern repetition for the classification process. Further,

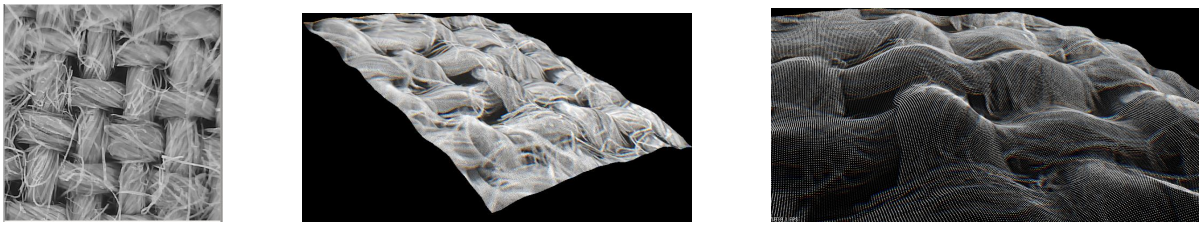

Figure 9. The albedo (left), the surface three-dimensional point cloud with albedo (middle) and a close view of the point cloud (right) of a Yuta fabric.

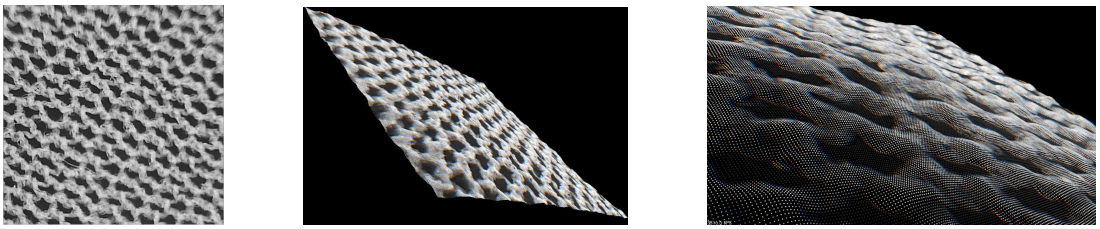

Figure 10. The albedo (left), the surface three-dimensional point cloud with albedo (middle) and a close view of the point cloud (right) of an elastic net.

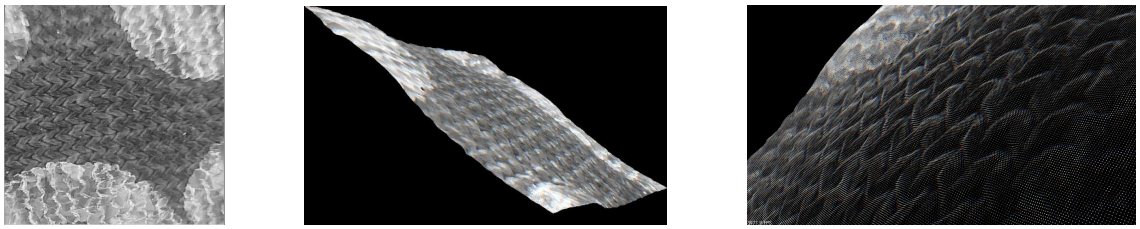

Figure 11. The albedo (left), the surface three-dimensional point cloud with albedo (middle) and a close view of the point cloud (right) of a Lurex fabric.

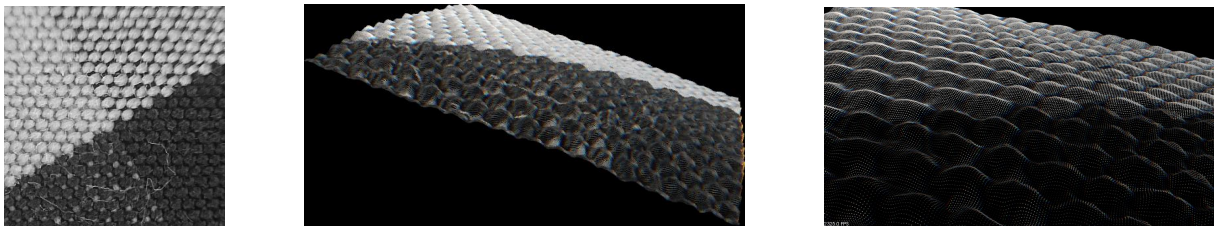

Figure 12. The albedo (left), the surface three-dimensional point cloud with albedo (middle) and a close view of the point cloud (right) of a cotton fabric.

the depth of field is adequate to reconstruct this coarse fabric without focus issues. This type of fabric presents one of the largest differentiations in depth and thus it is of great importance that the developed system can fully address its depth profile. Similarly, in Fig. 10, is presented another coarse fabric. This time, however, its depth profile is much smaller than what it is in Yuta. The net pattern of this elastic non-woven fabric has been reconstructed, preserving all the details of its structural features.

Two examples of fabrics with denser structure are presented in Fig. 11 and Fig. 12. The first one has been acquired from a Lurex cloth, which belongs to the embroidery category and presents metallic color patches. The second case comes from a cotton fabric with 1×1 plain weave pattern. The developed system successfully reconstructed both of these fabric types, as it can be observed in the corresponding figures. However, what is of great importance in these examples, is that the color variation of the textiles did not interfere with the reconstruction outcomes. Even in the case of the Lurex fabric, where metallic color patches are used, the developed system captured images with minimum highlights.

Although the field of view of the system is relatively small and the cylindrical enclosure ensures that the inspected surface is adequately flat for the shallow depth of field, there exist cases where the fabric presents a non-flat surface. If the height of the fabric wrinkle is small enough not to cause focus problems, then the system can successfully reconstruct the pattern, even if it is not on a flat surface. Such a case is shown in Fig. 13, where an example of a Taffeta fabric is presented, which belongs to the embroidery category with a plain weave pattern.

The system was finally tested on fabrics characterized by very fine structure, as those presented in Fig. 14 and Fig. 15. The first one comes from a lining Saglia fabric, with 1×1 plain weave pattern, whereas the second one comes from a micro-knit fabric, with purl knit pattern. Both these are fine fabrics with surface patterns characterized by micro-structural features. As it can be seen in both Fig. 14 and Fig. 15, the developed

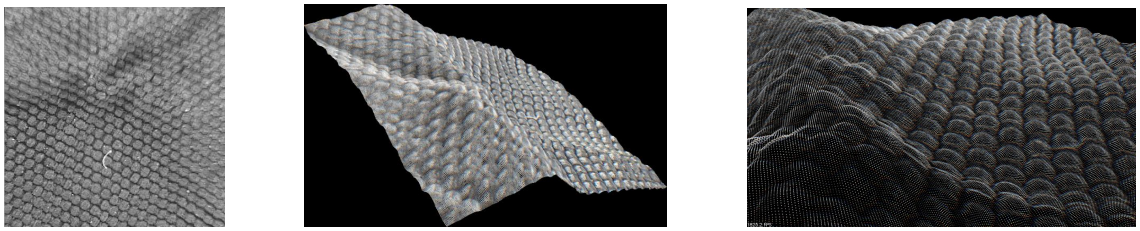

Figure 13. The albedo (left), the surface three-dimensional point cloud with albedo (middle) and a close view of the point cloud (right) of a Taffeta fabric.

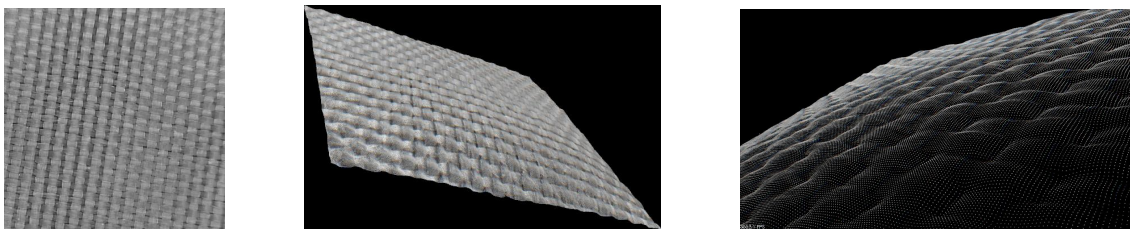

Figure 14. The albedo (left), the surface three-dimensional point cloud with albedo (middle) and a close view of the point cloud (right) of a lining Saglia fabric.

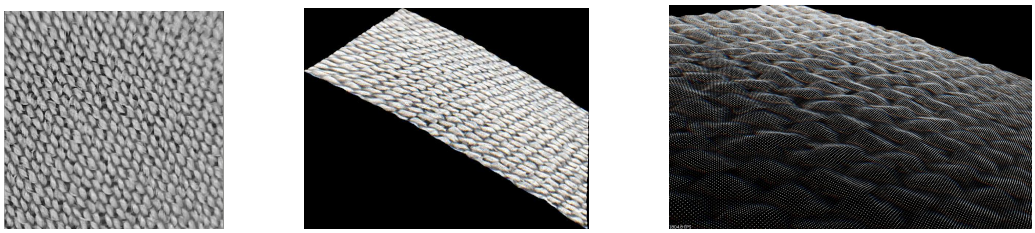

Figure 15. The albedo (left), the surface three-dimensional point cloud with albedo (middle) and a close view of the point cloud (right) of a micro knit fabric.

photometric stereo system reconstructed successfully the surface pattern of these fine fabrics, providing enough information for the classification process.

Besides the surface reconstruction of various fabrics, the developed system was also evaluated on other small objects. Among these objects, the most challenging cases were the reconstruction of a laser printed text in draft quality (150 dpi) and the texture of a 20 USD bill. The surface reconstruction of both these cases is presented in Fig. 16. The three-dimensional texture of the word "Treasurer" printed at the back of a 20 USD bill can be barely sensed through tactile sensation, yet it is clearly reconstructed with the developed photometric stereo system. Moreover, the printed word "CloPeMa" with draft quality and 6 pt font size by no means can be sensed as three-dimensional object. The developed system, however, managed to reconstruct the ink.

4. CONCLUSION

In this paper a lab prototype miniature photometric stereo system has been developed. The surface textures of various fabrics were reasonably reconstructed by using an off-the-self VGA resolution web-camera with manual focus. This system will be attached on the gripper of a robot which targets the solution of the "laundry problem", and the derived information will be used for the classification of the various garments according to their fabric type.

Since the targeted application is not a gauging one, the developed photometric stereo system has not been evaluated towards its reconstruction accuracy. The accuracy of the system will be determined during the subsequent

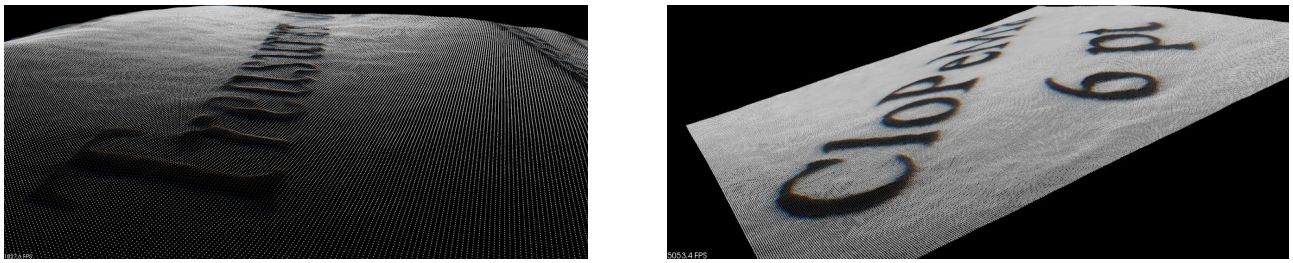

Figure 16. The word "Treasurer" printed at the back of a 20 USD bill (left) and a laser printed text in draft quality, 150 dpi (right).

stage of the classification, and will be defined as the accuracy in textile recognition. However, the visual inspection of the reconstructed surfaces suggests an increased accuracy in reconstruction depth profile. This will be further increased by revisiting the used photometric stereo algorithm and modifying it to incorporate close-range imaging and illumination. Moreover, the approximation of the textiles as being Lambertian surfaces will be also further investigated for its validity. In its current form, however, the preliminary results presented in this paper are comparable to the results available in literature, from systems much larger and equipped with high-end CCD cameras of several megapixels resolution.[16]

Future works also include mounting the module on the robot gripper and developing the communication interface between the robot controller and the photometric stereo system. This will also evaluate the focus measure that is used to estimate the image plane in totally uncontrolled environment.

The developed miniature device can also find use in numerous other applications. Its small size and the fact that the illumination spectra can be adjusted according to the application, make it a very promising tool for applications with space restrictions, like the quality control in production lines or scene interpretation based on structural information, or in applications where easiness in operation and light-weight are required, like those in the Biomedical imaging field, and especially in dermatology.

ACKNOWLEDGMENTS

This work is supported by the EU STREP Project "Clothes Perception and Manipulation", ICT-288553.

REFERENCES

[1] Miller, S., van den Berg, J., Fritz, M., Darrell, T., Goldberg, K., and Abbeel, P., "A geometric approach to robotic laundry folding," *Int. J. Robot. Res.* **31**(2), 249–267 (2012).

[2] Hu, J. and Xin, B., "Image based modelling and analysis of textile materials," in [*Integrated image and graphics technologies*], Zhang, D. D., Kamel, M., and Baciu, G., eds., 283–307, Kluwer Academic Publishers, Norwell, MA, USA (2004).

[3] Llado, X., Petrou, M., and Mart, J., "Surface texture recognition by surface rendering," *Opt. Eng.* **44**(3), 037001–037001–16 (2005).

[4] Woodham, R. J., "Photometric method for determining surface orientation from multiple images," *Opt. Eng.* **19**(1), 191139–191139 (1980).

[5] Barsky, S. and Petrou, M., "The 4-source photometric stereo technique for three-dimensional surfaces in the presence of highlights and shadows," *IEEE T. Pattern Anal.* **25**(10), 1239–1252 (2003).

[6] Basri, R., Jacobs, D., and Kemelmacher, I., "Photometric stereo with general, unknown lighting," *Int. J. Comput. Vision* **72**, 239–257 (2007).

[7] Hernandez, C., Vogiatzis, G., Brostow, G., Stenger, B., and Cipolla, R., "Non-rigid photometric stereo with colored lights," in [*Computer Vision, 2007. ICCV 2007. IEEE 11th International Conference on*], 1–8 (2007).

[8] Argyriou, V. and Petrou, M., "Chapter 1 photometric stereo: An overview," in [*Advances in Imaging and Electron Physics*], Hawkes, P. W., ed., *Advances in Imaging and Electron Physics* **156**, 1 – 54, Elsevier (2009).

[9] Bony, A., Bringier, B., and Khoudeir, M., "Accurate image quantization adapted to multisource photometric reconstruction for rough textured surface analysis," *J. Opt. Soc. Am. A* **30**, 518–526 (Mar 2013).

[10] Miyazaki, D., Shigetomi, T., Baba, M., Furukawa, R., Hiura, S., and Asada, N., "Polarization-based surface normal estimation of black specular objects from multiple viewpoints," in [*3D Imaging, Modeling, Processing, Visualization and Transmission (3DIMPVT), 2012 Second International Conference on*], 104–111 (2012).

[11] Beljan, M., Ackermann, J., and Goesele, M., "Consensus multi-view photometric stereo," in [*Pattern Recognition*], Pinz, A., Pock, T., Bischof, H., and Leberl, F., eds., *Lecture Notes in Computer Science* **7476**, 287–296, Springer Berlin Heidelberg (2012).

[12] Higo, T., Matsushita, Y., Joshi, N., and Ikeuchi, K., "A hand-held photometric stereo camera for 3-d modeling," in [*Computer Vision, 2009 IEEE 12th International Conference on*], 1234–1241 (2009).

[13] Broadbent, L., Emrith, K., Farooq, A., Smith, M., and Smith, L., "2.5d facial expression recognition using photometric stereo and the area weighted histogram of shape index," in [*RO-MAN, 2012 IEEE*], 490–495 (2012).

[14] Hansen, M. F., Atkinson, G. A., Smith, L. N., and Smith, M. L., "3d face reconstructions from photometric stereo using near infrared and visible light," *Comput. Vis. Image Underst.* **114**(8), 942 – 951 (2010).

[15] Zafeiriou, S., Atkinson, G., Hansen, M., Smith, W., Argyriou, V., Petrou, M., Smith, M., and Smith, L., "Face recognition and verification using photometric stereo: The photoface database and a comprehensive evaluation," *IEEE T. Inf. Foren. Sec.* **8**(1), 121–135 (2013).

[16] Johnson, M. K., Cole, F., Raj, A., and Adelson, E. H., "Microgeometry capture using an elastomeric sensor," *ACM Transactions on Graphics (Proc. ACM SIGGRAPH)* **30**(4), 46:1–46:8 (2011).

[17] Smith, L., Smith, M., Farooq, A., Sun, J., Ding, Y., and Warr, R., "Machine vision 3d skin texture analysis for detection of melanoma," *Sensor Rev.* **31**, 111 –119 (2011).

[18] Yang, X. and Huang, X., "Evaluating fabric wrinkle degree with a photometric stereo method," *Text. Res. J.* **73**(5), 451–454 (2003).

[19] Frankot, R. and Chellappa, R., "A method for enforcing integrability in shape from shading algorithms," *IEEE T. Pattern Anal.* **10**(4), 439–451 (1988).

[20] Drbohlav, O. and Chantler, M., "On optimal light configurations in photometric stereo," in [*Computer Vision, 2005. ICCV 2005. Tenth IEEE International Conference on*], **2**, 1707–1712 Vol. 2 (2005).

[21] Horn, B. K. P. and Brooks, M. J., eds., [*Shape from shading*], MIT Press, Cambridge, MA, USA (1989).

[22] Forsyth, D. A. and Ponce, J., [*Computer vision: a modern approach*], Prentice Hall Professional Technical Reference (2002).

[23] Santos, A., Ortiz De Solorzano, C., Vaquero, J. J., Pena, J. M., Malpica, N., and Del Pozo, F., "Evaluation of autofocus functions in molecular cytogenetic analysis," *J. Microsc.* **188**(3), 264–272 (1997).

[24] Nanda, H. and Cutler, R., "Practical Calibrations For A Real-Time Digital Omnidirectional Camera," in [*Proceedings of CVPR, Technical Sketch*], (2001).

[25] Yang, G. and Nelson, B., "Wavelet-based autofocusing and unsupervised segmentation of microscopic images," in [*Intelligent Robots and Systems, 2003. (IROS 2003). Proceedings. 2003 IEEE/RSJ International Conference on*], **3**, 2143–2148 vol.3 (2003).

[26] Geusebroek, J.-M., Cornelissen, F., Smeulders, A. W., and Geerts, H., "Robust autofocusing in microscopy," *Cytometry* **39**(1), 1–9 (2000).